Supporting Information

Shih et al. 10.1073/pnas.1323852111

SI Materials and Methods

Mice. Interleukin-23 receptor deficient (*IL-23r*$^{-/-}$), Interleukin-23 subunit p19 deficient (*IL-23p19*$^{-/-}$), Interleukin-22 deficient (*IL-22*$^{-/-}$), Interleukin-17F deficient (*IL-17f*$^{-/-}$), Interleukin-17 receptor C deficient (*IL-17rc*$^{-/-}$), recombination activating gene 2 deficient (*Rag2*$^{-/-}$), *IL-23r*$^{-/-}$*Rag2*$^{-/-}$, and Interleukin-2 receptor gamma chain deficient (*IL-2rγ*$^{-/-}$)*Rag2*$^{-/-}$ mice were generated as previously described (1–4). When analyzing intestinal microbiota composition in mice, colonic stool samples were collected immediately after euthanizing the mice. Fecal samples were kept frozen until subjected to bacterial DNA purification. Because segmented filamentous bacteria dysregulation in *Il-23r*$^{-/-}$ mice was consistently observed in the comparisons of cousins, littermates, and cofostered animals in Figs. 2 and 3, cousins of experimental animals were blindly assigned to different experimental groups and mice in different groups were not cohoused after the initiation of the studies. Mice from Genentech, Inc. were used for experiments, with the exceptions that Taconic WT mice were used in Figs. 4 and 5*B* and Jackson Laboratory WT mice were used in Fig. 5*B*. Mice aged 6 to 12 wk were used in this study unless otherwise indicated. All experiments were approved by the Institutional Animal Care and Use Committee of Genentech, Inc.

SEM. SEM was performed on 0.5-cm pieces of the terminal ileum. The terminal ileum was cut open, fixed in 2.5% glutaraldehyde and 2% paraformaldehyde in 0.1 M sodium cacodylate buffer (pH 7.2) for 2 h, and postfixed with 1% osmium tetroxide for 2 h at room temperature. The samples were then stained with 1% uranyl acetate for 2 h and dehydrated through a series of ethanol (50%, 70%, 90%, 95%, and 100%), followed by three changes in 100% hexamethyldisilazane. Finally, the samples were mounted on SEM stubs, air-dried, and coated with 5-nm palladium-gold using a HUMMER XP Sputter Coater (ANATECH LTD). The samples were imaged with an FEI XL30 ESEM in secondary electron mode at 5–10 kV and at a working distance of about 9 mm.

Assessment of Intestinal Inflammation. *Rag2*$^{-/-}$ or *Il23r*$^{-/-}$*rag2*$^{-/-}$ mice were monitored for weight loss and killed by CO_2 asphyxiation 4 wk after CD4$^+$ T-cell reconstitution. At the time of death, mouse colons were removed and flushed, the length was measured from rectum to cecum, and the colon mass was recorded. Colitis severity was macroscopically scored on a scale of 0–5, with 0 and 5 representing a normal colon and severe colitis, respectively.

Lamina Propria Leukocyte Isolation, ex Vivo Stimulation. Colons or distal small intestine were separated from mesentery, and Peyer's patches were carefully excised. Intestines were opened longitudinally and washed with HBSS buffer containing 2% FBS. Epithelial cells were separated from the lamina propria by incubating intestinal pieces in HBSS containing 5 mM EDTA and β-Mercaptoethanol for 40 min at 37 °C. Lamina propria tissue was washed with HBSS, diced into 1-mm pieces, and digested in a solution of 0.1 mg/mL Liberase (Roche), 0.15 mg/mL DNase (Roche), and 5% FBS for 30 min at 37 °C. Lamina propria leukocytes were washed with RPMI and collected for stimulation and FACS analysis.

Flow Cytometry. Antibodies used were purchased from either BD Pharmingen or eBioscience. Cell surfaces were stained with following antibodies: CD45 (30-F11), CD4 (RM4-5), TCR-β (H57-597), CD3 (17A2), CD25 (3C7), CD45Rb (16A), CD11b (M1/70), Gr1 (RB6-8C5), Thy1 (53-2.1), CD11c (HL3), CD11b (M1/70), TCR-γ/δ (GL3), CD8α (53-6.7), B220 (RA3-6B2), Ter119, SiglecF (E50-2440), NK1.1 (PK136), FcεR1 (MAR1), CD49b (DX5), and F4/80 (BM8). For intracellular staining, cells were fixed with Foxp3 staining buffer or fixation buffer (eBioscience) per the manufacturer's instructions and stained with the following antibodies: IL-17A (eBio17B7), IFN-γ (XMG1.2), IL-22 (1H8PWSR), or RAR-related orphan receptor-γ (Ror-γ; B2D). Before staining, all cell preparations were blocked with anti-mouse CD16/32 (Fc block) for 10 min. Cells were stained with live/dead fixable dye (Invitrogen) to exclude dead cells from analysis, and isotype controls were used to distinguish positive from negative staining populations. Cells were acquired using a Becton Dickinson LSR II flow cytometer, and flow cytometric data were analyzed with FlowJo software (Tree Star Software).

Bacterial Abundance Quantitation by 16S Ribosomal RNA Metagenomic Sequencing. Bacteria genomic DNA was isolated from colonic intestinal stool by means of a QIAamp DNA Stool Mini Kit (Qiagen). Metagenomic sequencing and data analysis were performed by Second Genome. Briefly, DNA samples were amplified with primers targeting V4 regions of 16S genes and sequenced using MiSeq technology (Illumina). Sequence analysis was performed using the QIIME pipeline and searched against the Greengenes reference database. Operational taxonomic unit (OTU) data were generated with 97% identity, and relative abundances of OTUs were calculated in units of sequences in an OTU per millions of sequences in a sample. Significant differences in OTU abundance were evaluated with $P < 0.05$ by the Student *t* test. Quantitative PCR analysis was performed with an ABI real-time PCR system detecting SyBR (Applied Biosystems) signal. Quantitation of bacteria abundance was calculated by the threshold cycle (ΔCt) method and normalized to stool mass. Bacteria quantity was presented as relative fold change compared with control samples in each experiment. Primers and PCR conditions used were as described (5, 6) and are listed in Table S3.

Gene Expression Analyses. Distal small intestine, a 10-cm segment close to the cecum, was excised and preserved in RNAlater (Qiagen). Tissues were homogenized with a TissueLyser Bead Dispenser System (Qiagen), and RNA was purified by means of an RNeasy Mini Kit (Qiagen) per the manufacturer's protocol. Isolated RNA was DNase-treated (Ambion) and reverse-transcribed by means of an iScript cDNA Synthesis Kit (Bio-Rad). Gene expression was assessed by quantitative real-time PCR with a TaqMan Detection System (Applied Biosystems) using the probes listed in Table S4. Signals were normalized to *Rpl19* mRNA expression and expressed as fold induction relative to the basal level.

Microbiota Transplantation. Fecal pellets were collected from ileum and cecum of donors and homogenized in PBS. Two hundred microliters of suspension was administered orally to recipients immediately.

1. Cox JH, et al. (2012) Opposing consequences of IL-23 signaling mediated by innate and adaptive cells in chemically induced colitis in mice. *Mucosal Immunol* 5(1):99–109.
2. Ghilardi N, et al. (2004) Compromised humoral and delayed-type hypersensitivity responses in IL-23-deficient mice. *J Immunol* 172(5):2827–2833.
3. Zheng Y, et al. (2007) Interleukin-22, a T(H)17 cytokine, mediates IL-23-induced dermal inflammation and acanthosis. *Nature* 445(7128):648–651.
4. Tang T, et al. (2010) A mouse knockout library for secreted and transmembrane proteins. *Nat Biotechnol* 28(7):749–755.
5. Barman M, et al. (2008) Enteric salmonellosis disrupts the microbial ecology of the murine gastrointestinal tract. *Infect Immun* 76(3):907–915.
6. Atarashi K, et al. (2011) Induction of colonic regulatory T cells by indigenous Clostridium species. *Science* 331(6015):337–341.

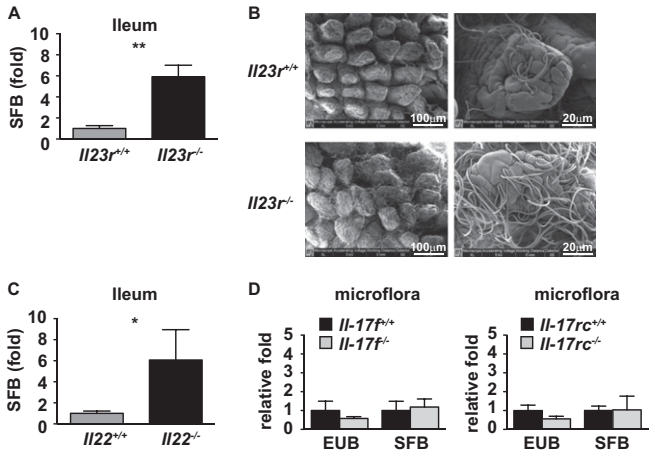

Fig. S1. IL-23, but not IL-17, is genetically required to control segmented filamentous bacteria (SFB) colonization. (*A*) Quantitative PCR (qPCR) analysis comparing the abundance of SFB in feces collected from WT and *Il-23r*$^{-/-}$ ileum. (*B*) SEM of terminal ileum of WT and *Il-23r*$^{-/-}$ mice. The increased presence of filamentous bacteria resembling the morphology of SFB was shown in *Il-23r*$^{-/-}$ mice. [Scale bars: 100 μm (*Left*) and 20 μm (*Right*).] (*C*) qPCR analysis comparing the abundance of SFB in feces collected from WT and *Il-22*$^{-/-}$ ileum. (*D*) qPCR analysis of intestinal bacteria quantity in mice with the indicated genotypes and their respective littermate controls. EUB, total bacteria. *$P < 0.05$; **$P < 0.01$.

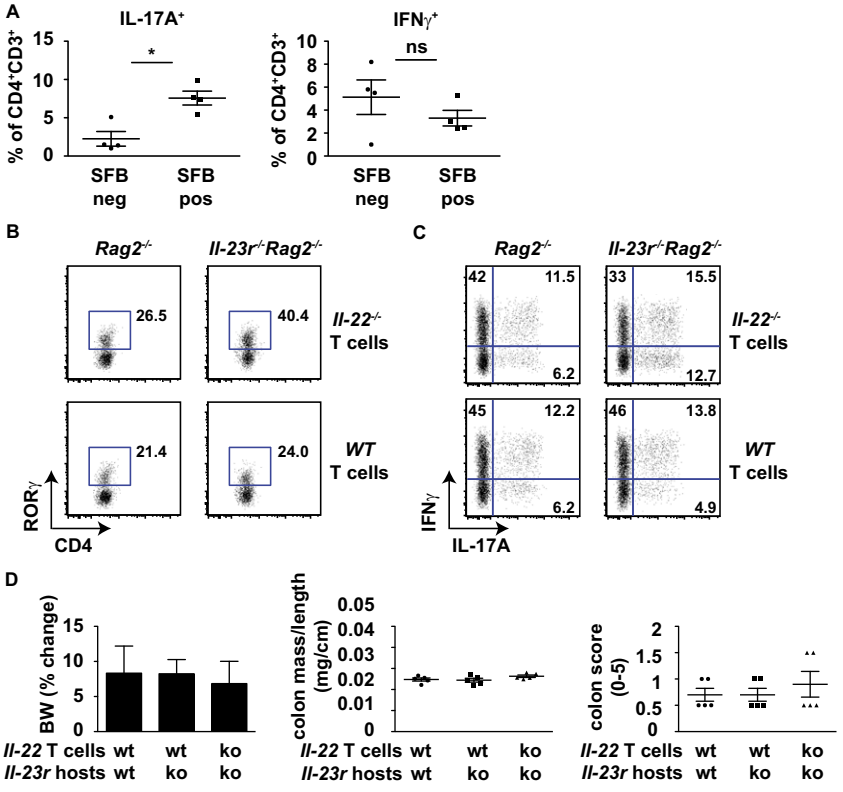

Fig. S2. IL-22 suppresses local Th17 responses. (*A*) Statistical analyses comparing IL-17–producing (*Left*) and IFN-γ–producing colonic CD4$^+$CD3$^+$ T cells in SFB-negative vs. SFB-positive *rag1*$^{-/-}$ mice 2 wk after CD4$^+$ T-cell adoptive transfer. This experiment was performed at the University of Pittsburgh, using *rag1*$^{-/-}$ recipient mice, whereas all other experiments were done at Genentech, Inc., using *rag2*$^{-/-}$ mice. We suspect that a difference in background microflora between the facilities and mouse strains is the reason for the generally lower percentages of IFN-γ$^+$ cells. (*B* and *C*) Transcription factor and cytokine expression in WT or *Il-22*$^{-/-}$ CD4$^+$ T cells adoptively transferred into *Rag2*$^{-/-}$ or *Il-23r*$^{-/-}$*Rag2*$^{-/-}$ mice were assessed. Representative flow cytometry plots on gated CD4$^+$TCR-β$^+$ lymphocytes derived from colonic lamina propria are shown. Numbers indicate the frequency of transcription factor- or cytokine-expressing cells. (*D*) *Rag2*$^{-/-}$ or *Il23r*$^{-/-}$*rag2*$^{-/-}$ mice were reconstituted with WT or *IL-22*$^{-/-}$ CD4$^+$ T cells, and body weight change (*Left*), colon mass vs. length ratio (*Center*), and colon score (*Right*) were analyzed 4 wk after reconstitution. neg, negative; ns, not significant; pos, positive.

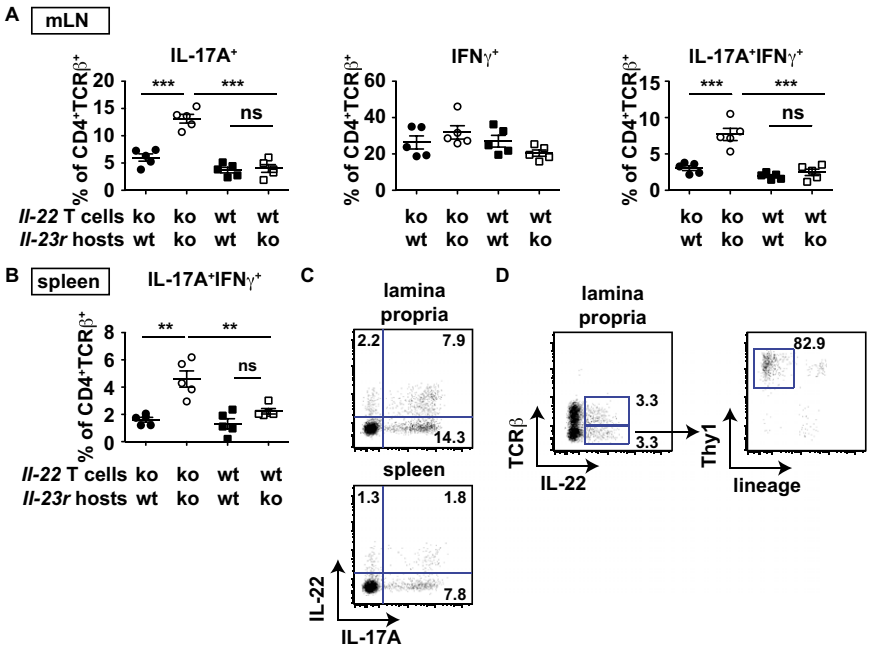

Fig. S3. IL-22 suppresses systemic Th17 responses. (*A* and *B*) Statistical analyses of cytokine expression in WT or *Il-22*$^{-/-}$ CD4$^+$ T cells adoptively transferred into *Rag2*$^{-/-}$ or *Il-23r*$^{-/-}$*Rag2*$^{-/-}$ mice assessed 14 d after reconstitution. Gated CD4$^+$TCR-β$^+$ lymphocytes derived from mesenteric lymph node (mLN) (*A*) or spleen (*B*) were analyzed. (*C*) Representative fluorescence-activated cell sorting (FACS) plots revealing the frequency of IL-17A and IL-22 producing CD4$^+$TCR-β$^+$ T cells in *Rag2*$^{-/-}$ recipients adoptively transferred with WT CD4$^+$ T cells. (*D*) Representative FACS plots showing the frequency of IL-22 producing TCR-β$^+$ and TCR-β$^-$ cells in the lamina propria 2 wk after CD4$^+$ T-cell reconstitution in *rag2*$^{-/-}$ recipients (*Left*). IL-22–producing innate lymphoid cells were further revealed by TCR-β$^-$ cells gated on Thy1$^+$lineage$^-$ cells (Thy1$^+$ CD11c$^-$ CD11b$^-$ TCR-γ/δ$^-$ CD8α$^-$ B220$^-$ Gr1$^-$ Ter119$^-$ SiglecF$^-$ NK1.1$^-$ FcεR1$^-$ CD49b$^-$ F4/80$^-$). $^{**}P < 0.01$; $^{***}P < 0.001$.

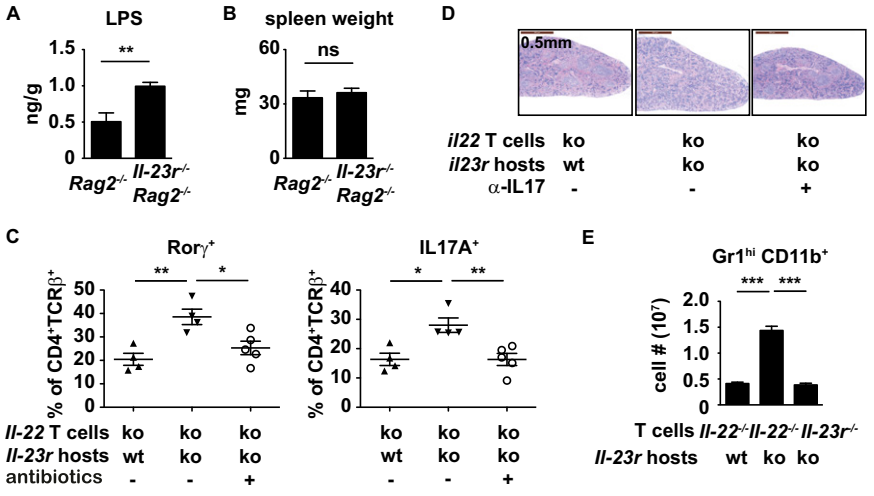

Fig. S4. Defective containment of commensal microflora leads to IL-17–dependent splenomegaly. Comparisons of endotoxin contents in liver homogenates (*A*) and spleen weights (*B*) in *Rag2*$^{-/-}$ vs. *Il-23r*$^{-/-}$*Rag2*$^{-/-}$ mice. (*C*) Statistical analysis on Ror-γ– and IL-17A–expressing CD4$^+$TCR-β$^+$ T cells in *Rag2*$^{-/-}$ or *Il-23r*$^{-/-}$*Rag2*$^{-/-}$ recipients adoptively transferred with *Il-22*$^{-/-}$ CD4$^+$ T cells. Mice were maintained with regular water or orally fed with a mixture of antibiotics in the drinking water as indicated. (*D*) Representative H&E staining on spleens derived from anti–IL-17 or control antibody-treated *Rag2*$^{-/-}$ or *Il-23r*$^{-/-}$*Rag2*$^{-/-}$ mice reconstituted with *Il-22*$^{-/-}$ CD4$^+$ T cells. (Scale bar: 500 μm.) (*E*) Splenic Gr1^{hi}CD11b$^+$ cell numbers in *Rag2*$^{-/-}$ or *Il-23r*$^{-/-}$*Rag2*$^{-/-}$ mice reconstituted with *Il-22*$^{-/-}$ or *Il-23r*$^{-/-}$ CD4$^+$ T cells. $^*P < 0.05$; $^{**}P < 0.01$; $^{***}P < 0.001$.

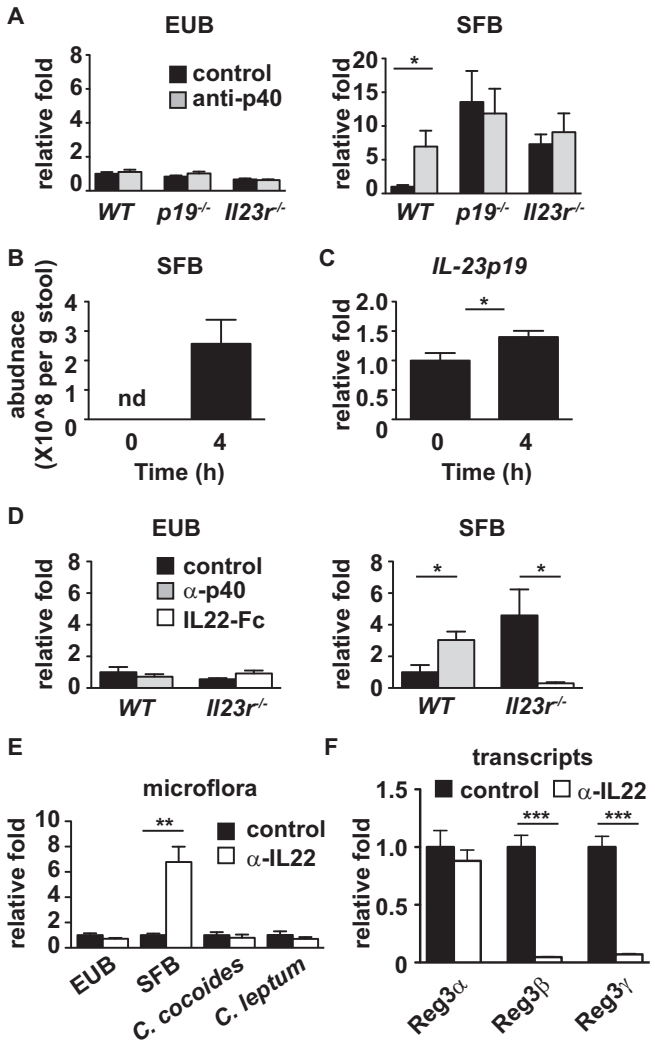

Fig. S5. SFB abundance can be modulated by pharmacological agents perturbing the IL-23/IL-22 pathway. (*A*) qPCR analysis quantitating bacteria abundance in mice treated with 100 μg of anti-p40 antibody. qPCR analysis of intestinal SFB abundance (*B*) and ileal *IL-23p19* gene expression (*C*) in Jackson Laboratory WT mice before and 4 h after fecal transplantation of SFB-containing feces from Taconic mice. nd, not detectable. qPCR analysis quantitating bacteria abundance (EUB, SFB, *Clostridium coccoides*, and *Clostridium leptum*) in mice treated with 50 μg of IL-22–Fc (*D*) or 150 μg of anti–IL-22 antibody (*E*). (*F*) Gene expression analysis of Reg3 family members in ileal tissues collected from control mice or mice treated with anti–IL-22. Signals were normalized to their respective bacterial abundance or transcript quantities in control IgG-treated mice. $*P < 0.05$; $**P < 0.01$; $***P < 0.001$.

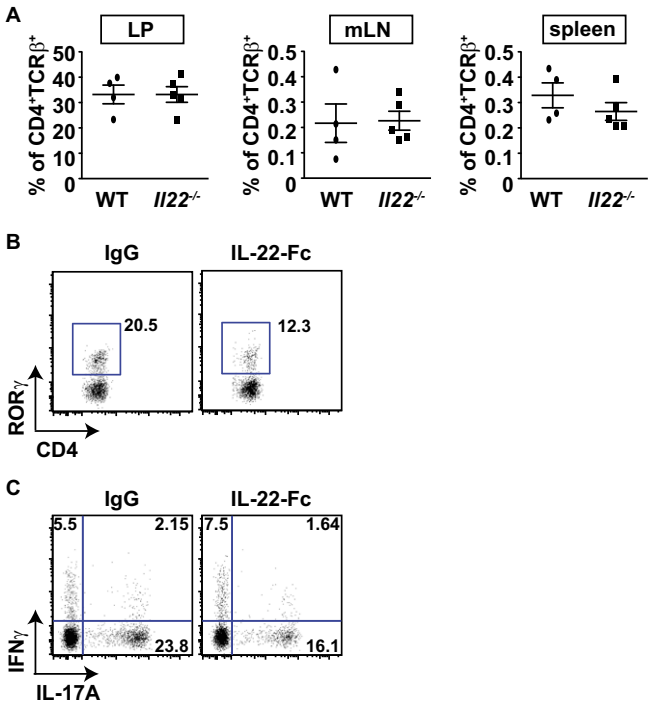

Fig. S6. IL-22–Fc treatment suppresses Th17 development in WT mice. (*A*) Statistical comparisons of IL-17–expressing $CD4^+TCR\text{-}\beta^+$ cells in WT vs. *Il-22*$^{-/-}$ cells harvested from small intestine lamina propria (LP; *Left*), mLN (*Center*), or spleen (*Right*). Expression of Ror-γ (*B*) and IL-17A and IFN-γ (*C*) in live $CD45^+$ cells gated on $CD4^+TCR\text{-}\beta^+$ cells isolated from the ileum LP from WT mice treated with 30 μg of control antibody or IL-22–Fc for 1 wk.

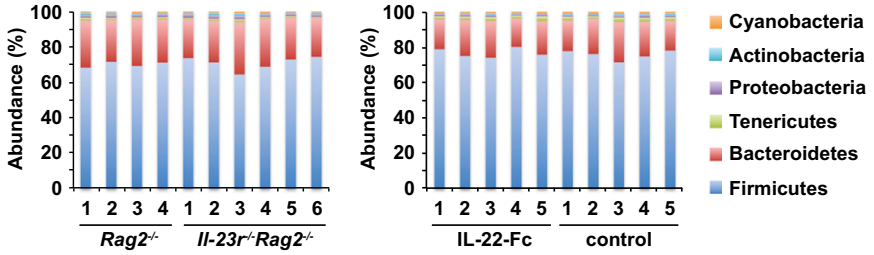

Fig. S7. 16s rRNA gene sequencing to identify IL-23/IL-22–regulated microbiota. 16s rRNA gene sequencing of intestinal fecal contents collected from the indicated gene-deficient mice or WT mice treated with 50 μg of IL-22–Fc or control antibody. Bar graphs reveal compositions of intestinal commensal microbiota compared between *Rag2*$^{-/-}$ and *Il-23r*$^{-/-}$*Rag2*$^{-/-}$ mice (*Left*) or mice treated with IL-22–Fc and IgG (*Right*) at the family level.

Table S1. List of OTUs dysregulated in *Il-23r*$^{-/-}$*Rag2*$^{-/-}$ mice vs. *Rag2*$^{-/-}$ mice

OTU	Phylum	Class	Order	Family
215086	Firmicutes	Clostridia	Clostridiales	Catabacteriaceae
216356	Firmicutes	Clostridia	Clostridiales	Catabacteriaceae
383716	Firmicutes	Clostridia	Clostridiales	Clostridiaceae
314786	Firmicutes	Clostridia	Clostridiales	Lachnospiraceae
372432	Firmicutes	Clostridia	Clostridiales	Lachnospiraceae
411254	Firmicutes	Clostridia	Clostridiales	Lachnospiraceae
204782	Firmicutes	Clostridia	Clostridiales	Lachnospiraceae
233664	Bacteroidetes	Bacteroidia	Bacteroidales	Rikenellaceae
234443	Bacteroidetes	Bacteroidia	Bacteroidales	Rikenellaceae
385442	Bacteroidetes	Bacteroidia	Bacteroidales	Rikenellaceae II
188495	Bacteroidetes	Bacteroidia	Bacteroidales	Rikenellaceae II
214403	Bacteroidetes	Bacteroidia	Bacteroidales	Rikenellaceae II
177425	Bacteroidetes	Bacteroidia	Bacteroidales	Rikenellaceae II
193038	Bacteroidetes	Bacteroidia	Bacteroidales	Rikenellaceae II
266075	Bacteroidetes	Bacteroidia	Bacteroidales	Rikenellaceae II
457356	Bacteroidetes	Bacteroidia	Bacteroidales	Rikenellaceae II
209377	Bacteroidetes	Bacteroidia	Bacteroidales	Rikenellaceae II
407007	Firmicutes	Clostridia	Clostridiales	Ruminococcaceae
170926	Firmicutes	Clostridia	Clostridiales	Ruminococcaceae
396448	Firmicutes	Clostridia	Clostridiales	Ruminococcaceae
251289	Firmicutes	Clostridia	Clostridiales	Ruminococcaceae

Table S2. List of OTUs down-regulated by IL-22–Fc treatment in Taconic WT mice

OTU	Phylum	Class	Order	Family
383716	Firmicutes	Clostridia	Clostridiales	Clostridiaceae
304779	Firmicutes	Clostridia	Clostridiales	Clostridiaceae
305803	Firmicutes	Clostridia	Clostridiales	Lachnospiraceae
263865	Firmicutes	Clostridia	Clostridiales	Lachnospiraceae
323257	Firmicutes	Bacilli	Lactobacillales	Lactobacillaceae
329446	Firmicutes	Bacilli	Lactobacillales	Lactobacillaceae
179681	Bacteroidetes	Bacteroidia	Bacteroidales	Rikenellaceae II
386729	Bacteroidetes	Bacteroidia	Bacteroidales	Rikenellaceae II
261177	Bacteroidetes	Bacteroidia	Bacteroidales	Rikenellaceae II
385442	Bacteroidetes	Bacteroidia	Bacteroidales	Rikenellaceae II
199177	Bacteroidetes	Bacteroidia	Bacteroidales	Rikenellaceae II
420373	Bacteroidetes	Bacteroidia	Bacteroidales	Rikenellaceae II
374370	Bacteroidetes	Bacteroidia	Bacteroidales	Rikenellaceae II
169379	Bacteroidetes	Bacteroidia	Bacteroidales	Rikenellaceae II
177425	Bacteroidetes	Bacteroidia	Bacteroidales	Rikenellaceae II
333695	Bacteroidetes	Bacteroidia	Bacteroidales	Rikenellaceae II
214403	Bacteroidetes	Bacteroidia	Bacteroidales	Rikenellaceae II
162913	Bacteroidetes	Bacteroidia	Bacteroidales	Rikenellaceae II
292591	Bacteroidetes	Bacteroidia	Bacteroidales	Rikenellaceae II
196985	Bacteroidetes	Bacteroidia	Bacteroidales	Rikenellaceae II
299687	Bacteroidetes	Bacteroidia	Bacteroidales	Rikenellaceae II
322059	Bacteroidetes	Bacteroidia	Bacteroidales	Rikenellaceae II
209377	Bacteroidetes	Bacteroidia	Bacteroidales	Rikenellaceae II
517722	Bacteroidetes	Bacteroidia	Bacteroidales	Rikenellaceae II
300748	Bacteroidetes	Bacteroidia	Bacteroidales	Rikenellaceae II
296496	Firmicutes	Clostridia	Clostridiales	Ruminococcaceae
213870	Firmicutes	Clostridia	Clostridiales	Ruminococcaceae
209845	Firmicutes	Clostridia	Clostridiales	Ruminococcaceae
257881	Firmicutes	Clostridia	Clostridiales	Ruminococcaceae
257881	Cyanobacteria	4C0d-2	YS2	Unclassified
342685	Tenericutes	Mollicutes	RF39	Unclassified

Table S3. List of primers used in bacteria quantitation

Bacteria species	Name	Sequence
All bacteria	Uni340F	ACTCCTACGGGAGGCAGCAGT
All bacteria	Uni514R	ATTACCGCGGCTGCTGGC
Clostridium coccoides	Uni338F	ACTCCTACGGGAGGCAGC
C. coccoides	C.coc491R	GCTTCTTAGTCAGGTACCGTCAT
Clostridium leptum	sg-CleptF	GCACAAGCAGTGGAGT
C. leptum	sg-CleptR	CTTCCTCCGTTTTGTCAA
SFB	SFB736F	GACGCTGAGGCATGAGAGCAT
SFB	SFB844R	GACGGCACGGATTGTTATTCA

Table S4. List of primers used in quantitative gene expression

Gene	Sequence
mRPL19 (F)	AGCGCATCCTCATGGAGC
mRPL19 (R)	GTCAGCCAGGAGCTTCTTGC
mRPL19 probe	GCCTTGTCTGCCTTCAGCTTGTGGA
mReg3α (F)	TTTGTGTCCTCCTTGGTGAA
mReg3α (R)	GTTGTTGACCCATTGTTGGA
mReg3α probe	CCAAGACATCTGGATTGGGCTCC
mReg3β (F)	ATGGCTCCTACTGCTATGCC
mReg3β (R)	GTGTCCTCCAGGCCTCTTT
mReg3β probe	TGATGCAGAACTGGCCTGCCA
mReg3γ (F)	ATGGCTCCTATTGCTATGCC
mReg3γ (R)	GATGTCCTGAGGGCCTCTT
mReg3γ probe	TGGCAGGCCATATCTGCATCATACC
IL-23p19	4331182 (Life Technologies)

F, forward; mReg3, murine Regenerating islet-derived protein 3; mRPL19, murine ribosomal protein L19; R, reverse.